JAAS

PAPER

Cite this: *J. Anal. At. Spectrom.*, 2019, **34**, 1708

Optimization of lithium isotope analysis in geological materials by quadrupole ICP-MS

Xiao-Ming Liu * and Wenshuai Li*

Received 18th May 2019
Accepted 18th June 2019

DOI: 10.1039/c9ja00175a

rsc.li/jaas

This study develops and optimizes a new protocol to measure lithium isotope ratios using a single collector quadrupole inductively coupled plasma mass spectrometer (Q-ICP-MS) operated under hot plasma (1550 W) conditions with a sample–standard bracketing method. Our Q-ICP-MS method reduces sample consumption to 2.5 ng of Li and achieves a high long-term precision of 1.1‰ (2SD). This Q-ICP-MS method exhibits high matrix tolerance (Na/Li < 100), suitable for ng-sized and high-matrix geological samples. We also developed a dual-column system for Li separation, with large loading capacity (29.6 meq), complete recovery (~100%) and satisfactory purification (Na/Li m m^{-1} < 1), as well as a fixed elution range for Li fractions (28–60 mL). This new chromatography method has been applied to chemically diverse materials, producing consistent results. In addition, we report the Li isotope compositions of 13 geostandards, and our measurements agree well with reported data within analytical uncertainties. This study documents that Li element concentration and Li isotope composition can be routinely measured using a single collector ICP-MS, which is convenient and commercially affordable for future Li isotope research across the fields of Earth and Environmental Sciences.

Introduction

Recent studies have advanced our knowledge of lithium (Li) isotope geochemistry by documenting the Li isotope variations among geological reservoirs on Earth, and other bodies in the solar system.[1–4] Knowledge of Li isotope systematics provides a new tracer to understand various geological processes, such as silicate weathering,[5–7] hydrothermal alteration,[8–11] metamorphic dehydration,[12–14] temperature-driven diffusion[15–17] and source mixing.[18–20] Precise and accurate determination of Li isotope compositions in geological samples is crucial to expanding the application of Li isotopes. High-precision Li isotope measurements are usually performed by thermal ionization mass spectrometry (TIMS, 2SD = ±0.08–2.5‰)[21–24] and multicollector inductively coupled plasma mass spectrometry (MC-ICP-MS, 2SD = ±0.2–1.4‰).[25–31] However, these methods are susceptible to matrix-driven ionization suppression.[32] To minimize matrix-induced mass bias effects, previous studies highlighted the complete separation of Li from interfering elements.[33–35] Besides, TIMS and MC-ICP-MS techniques have multiple limitations. For example, TIMS methods usually require large sample consumption (>100 ng Li), with high procedural blanks (100 pg level Li) and instrumental fractionation.[23,24] Comparatively, MC-ICP-MS methods show low mass requirement (~2–40 ng Li),[25–30] but are sensitive to matrix interference.[36,37] Moreover, the low-level resistors of the Faraday cups exhibit low ion detection sensitivity, which makes it challenging to analyze samples with a super-low analyte concentration and high matrix.[25–27]

Early application of the quadrupole inductively coupled plasma mass spectrometer (Q-ICP-MS) demonstrated small sample requirement (down to 5 ng Li) and acceptable precision (2SD = ±1.0‰ at best).[38–40] Since the development of MC-ICP-MS in the first decade of the 21st century, few efforts have been focused on Q-ICP-MS. Thus, the most recent endeavor was undertaken by Misra and Froelich (2009).[42] Their method employed an older version of the Q-ICP-MS (Agilent™ 7500), and used cool plasma conditions for Li isotope analysis. They achieved sub-ng level Li requirement and high external precision (2SD = ±1.5‰) for seawater and natural carbonate samples. Since the instrument used is out of production, development and optimization of a new Q-ICP-MS instrument platform is needed. Moreover, a routine analytical method is important for the wider application of Li isotopes across the fields of Earth and Environmental Sciences.

Here we refine the Li column chemistry, and develop a simple analytical routine using an Agilent™ 7900 Q-ICP-MS for Li isotope analysis. Our chromatographic protocol aims to achieve low blanks, high loading capacity, 100% yield, and a fixed Li elution range. The instrumental setup developed has been optimized and confirmed to achieve high-precision Li isotope measurement (2SD = ±1.1‰) with low mass requirement. Our objective is to provide operational guidance for

Department of Geological Sciences, Plasma Mass Spectrometry Laboratory, University of North Carolina at Chapel Hill, 104 South Road, Mitchell Hall, Chapel Hill, NC 27599-3315, USA. E-mail: xiaomliu@unc.edu; wenshuai@live.unc.edu; Tel: +1 919 962 0675

scientists interested in Li isotope measurements in a convenient and commercially affordable way.

Materials and methods

All the experimental and analytical work in this study was conducted at the Plasma Mass Spectrometry (PMS) Laboratory at the University of North Carolina, Chapel Hill. Sample dissolution and column chemistry were carried out in Class 100 vertical laminar flow hoods. A full description of the proposed protocols and analysis techniques is given below.

Chemicals and standards

Ultrapure water (18.2 MΩ) was produced by de-ionization of reverse osmosis water using a Milli-Q water purification system (Direct-Q 3 UV, Merck Millipore™, Germany). High-purity nitric acid (HNO_3), hydrochloric acid (HCl) and hydrofluoric acid (HF) were purified in-house by double distillation in Savillex™ Teflon acid purification systems. The acids used were gravimetrically diluted to required molarities with MQ water. Lithium isotope standard IRMM-016,[42] available from the Institute for Reference Materials and Measurements (IRMM), was used as the bracketing standard.

For optimization of the isolation of lithium from various geological samples, 13 certified international reference materials with different Li contents and matrix/Li ratios were adopted in this study to evaluate the effect of matrix on column chemistry. The geostandards covering a large range of chemically diverse geological materials were processed and analyzed to assess the accuracy and procedural reproducibility. We purchased a limestone standard (NIST-SRM-1d) from the National Institute of Standards and Technology, a coral standard (JCP-1) from the Geological Survey of Japan, and a granodiorite (GSP-2), a continental flood basalt (BCR-2), an ocean island basalt (BHVO-2), a marine manganese nodule (NOD-A-1) and a marine shale (SBC-1) from the United States Geological Survey. We also obtained a basalt standard (JB-2) and a granite standard (JG-2) from the Geological Survey of Japan. In addition, we purchased three clay standards (kaolinite, KGa-2; illite, IMt-2; and montmorillonite, SWy-3) from the Clay Mineral Society and a seawater standard (NASS-7) from the National Research Council Canada. These standards have been widely used in Li isotope research and thus permit inter-laboratory comparisons.

Sample digestion

The entire sample digestion was performed at the Isotope Geochemical Laboratory at the University of North Carolina, Chapel Hill. Between 10 and 100 mg of standard powders were acid-digested with a HF–HNO_3 mixture (3 : 1 v/v) in 15 mL Savillex™ Teflon beakers and placed on a hotplate at temperatures exceeding 120 to 130 °C until total dissolution was achieved. The shale standard SBC-1 was treated with ultrapure H_2O_2 (Fisher Scientific™) to oxidize the organics. The samples were then dried, refluxed with aqua regia (3 : 1 M/M; conc. HNO_3 : conc. HCl) and placed on a hotplate at ~120 °C overnight. The drying operation was repeated, using the same amount of HCl until the solution became clear. After reaching dryness, the acquired residues were dissolved in 2% (v/v) nitric acid. All of the prepared samples were stored in Class 100 vertical laminar flow hoods (AirClean™ 600 PCR workstation). The acquired samples were dried and re-dissolved in 0.7 M HNO_3, ready for column chemistry.

Chromatography

For precise Li isotope measurement, it is crucial to thoroughly separate Li from other matrix elements, because the presence of matrix elements could generate spectral effects on Li isotopes. The common peak overlap in chromatography makes quantitative separation of Li from Na analytically challenging.[35] To ensure the matrix-matched principle on Li isotope measurement, Na should also be separated from Li, in particular for low sample size and high-matrix level geological samples (*e.g.*, seawater and brines). The designed chromatography was composed of two steps to ensure high sample loading and a fixed Li elution range (Table 1). The first step columns were Bio-Rad™ Econo-Pac (1.5 cm ID, polypropylene) columns and the second step columns were custom-made (0.6 cm ID, polypropylene) columns. All columns were loaded with a pre-cleaned cation-exchange resin, AG 50W-X8 resin (200–400 mesh size), which was successfully used to separate Li and K from natural samples.[28,29,42–46]

Our column protocol includes two steps, which allows Li to be isolated sufficiently from the matrices, with special optimization for ng-sized and high-matrix level geological samples. The main differences between this study and our previous study[35] are the size of the polypropylene column and the volume of the resin. The first step was for purifying Li with partial Na from most major and minor elements with 0.7 M HNO_3 through the fat column loaded with 17 mL resin. So, the total capacity of the wet resin is 29.6 meq (1.74 meq per mL wet capacity). This capacity meets the requirement for Li separation from geological samples with diverse matrix compositions. Columns were first cleaned with 100 mL 6 mol L^{-1} double-distilled HCl and then conditioned with 50 mL 0.7 mol L^{-1} double-distilled HNO_3. After centrifugation, the samples dissolved in 2 mL 0.7 mol L^{-1} HNO_3 were loaded onto the first columns. Matrix elements were eluted by adding 25 mL 0.7 mol L^{-1} HNO_3 and then pre-cuts were collected into acid-cleaned polypropylene tubes by adding 5 mL 0.7 mol L^{-1} HNO_3. Li fractions were recovered into acid-cleaned Teflon beakers using 50 mL 0.7 mol L^{-1} HNO_3. Post-cuts were also collected into additional acid-cleaned polypropylene tubes with 5 mL 0.7 mol L^{-1} HNO_3. The recovered Li was then dried and dissolved in 2 mL 0.2 mol L^{-1} HCl before being loaded onto the second column. The second column was used for separating Li from Na with 0.2 M HCl through the thin column packed with 3.4 mL resin.

All columns were first cleaned with 50 mL 6 mol L^{-1} double-distilled HCl and then conditioned with 20 mL 0.2 mol L^{-1} HCl. The samples in 2 mL 0.2 mol L^{-1} HCl were loaded onto the second columns. Matrix elements were eluted by adding 30 mL 0.2 mol L^{-1} HCl and pre-cuts were collected into acid-cleaned polypropylene tubes with 2 mL 0.2 mol L^{-1} HCl.

Table 1 Two-step chromatographic Li purification protocols

Details	Column 1	Column 2
Parameters	Fat column (ID = 1.5 cm, polypropylene, BioRed™ Econo-Pac) filled with 17 mL AG50-X8 200–400 mesh cation-exchange resin (wet)	Thin column (ID = 0.6 cm, polypropylene, custom-made) filled with 3.4 mL AG50-X8 200–400 mesh cation-exchange resin (wet)
Loading capacity	29.6 meq	5.9 meq
Resin cleaning	100 mL 6 mol L^{-1} HCl	50 mL 6 mol L^{-1} HCl
Conditioning	50 mL 0.7 mol L^{-1} HNO_3	20 mL 0.2 mol L^{-1} HCl
Sample loading	The samples are digested in 2.1 mL 0.7 mol L^{-1} HNO_3. After centrifuging the solution, 2 mL supernatant is loaded onto the fat columns	The samples are digested in 2 mL 0.2 mol L^{-1} HCl and then loaded onto the thin columns
Matrix elution	25 mL 0.7 mol L^{-1} HNO_3	30 mL 0.2 mol L^{-1} HCl
Pre-cut	5 mL 0.7 mol L^{-1} HNO_3 to monitor Li recovery	2 mL 0.2 mol L^{-1} HCl to monitor Li recovery
Li collection	50 mL 0.7 mol L^{-1} HNO_3	28 mL 0.2 mol L^{-1} HCl
Post-cut	5 mL 0.7 mol L^{-1} HNO_3 to monitor Li recovery	2 mL 0.2 mol L^{-1} HCl to monitor Li recovery
Resin regeneration	50 mL 6 mol L^{-1} HCl 50 mL MQ water	50 mL 6 mol L^{-1} HCl 50 mL MQ water

Subsequently, Li was recovered into acid-cleaned Teflon beakers using 28 mL 0.2 mol L^{-1} HCl. Post-cuts were collected into additional acid-cleaned polypropylene tubes by adding 2 mL 0.2 mol L^{-1} HCl. The recovered Li solutions were dried and converted to the nitrate matrix form. Afterward, aliquots of each of the samples were prepared in 2% HNO_3 (v/v) containing 0.5 ppb Li for Q-ICP-MS analyses. The total procedural blank is <0.004 ng. The final Na/Li ratio (m m^{-1}) in collections is less than 1, preventing the interference of Na^+ in Li isotope analysis.

Mass spectrometry

All isotope analyses were performed using an Agilent Technologies™ 7900, a single collector quadruple-ICP-MS at the Plasma Mass Spectrometry (PMS) Laboratory at the University of North Carolina, Chapel Hill. The instrumental settings for Li isotope ratio determination are summarized in Table 2, where both hot plasma (1550 W) and cool (600 W) plasma conditions were tested. We used an Agilent™ microflow self-aspirating 200 μL min^{-1} PFA nebulizer, quartz spray chamber, quartz torch and 2.5 mm internal diameter injector and S-lenses. We compared platinum and nickel cones and skimmers for carry-over effects and blanks, but did not observe any difference. Therefore, we adopted nickel cones for all Li isotope analyses. To achieve high signal stability and a low background, we optimized the nebulizer and make-up gas flow. To obtain equal numbers of ion counts for both Li isotopes, we used an integration time of 1 s and 12 s for ^7Li and ^6Li, respectively, roughly in inverse proportion to their natural isotope abundance. All tuning parameters are checked daily to maximize instrument sensitivity and stability. Each measurement included 1000 integrations of ^7Li and ^6Li measurement and was replicated between 5 and 8 times, followed by 3 minutes of washing to lower the Li signal to an insignificant level (<100 cps on ^7Li). The instrumental sensitivity was on average 250 000 cps on ^7Li for a 0.5 μg L^{-1} solution.

The discrepancy between measured and true Li isotope ratios may come from three factors: memory effects, instrumental mass bias, and matrix effects. Because of the low sample size (0.5 μg L^{-1}) and long washing time (180 s) adopted as the control of background levels, memory effects can be sufficiently mitigated. In particular, we used three washing reagents to ensure a thorough washout of Li: (i) 1% HF + 2% HNO_3 (v/v), (ii) 1% HNO_3 + 5% HCl (v/v) mixture, and (iii) 2% HNO_3 (v/v). Compared with the 2% HNO_3-only washing method, the blank was significantly decreased when adding 1% HF + 2% HNO_3 and 2% HNO_3 + 5% HCl. The blank signals for ^7Li (<10 cps, 0.1 s integration) were orders of magnitude lower compared with those of the 2% HNO_3-only washing procedure, which lowered the analytical uncertainties for our isotope ratios. Commonly, plasma-source mass spectrometry suffers from instrumental mass bias derived from preferential extraction and transmission of heavier ions over lighter ions.[41] We observed slight instrumental drifts in $^7Li/^6Li$ ratios with time (not shown here). So, we used the standard–sample–standard bracketing protocol to acquire precise Li isotope data. Here we express the Li isotope composition using δ^7Li, which is the per mil deviation from the NIST L-SVEC standard, defined as δ^7Li (‰, L-SVEC) = $[(^7Li/^6Li)_{sample}/(^7Li/^6Li)_{L\text{-}SVEC} - 1] \times 1000$. However, L-SVEC is no longer available and the IRMM-016 standard shows identical Li isotope composition. Therefore, we used IRMM-016 as the bracketing standard to correct for instrumental mass bias. After this correction and thorough washout between samples, the remaining δ^7Li drifts on the Q-ICP-MS could be attributed to matrix effects, which will be evaluated in detail next.

Results and discussion

Generalized chromatographic purification

Various single- and dual-column cation-exchange chromatographies have been described in the literature for Li isotope analysis.[25,27–30,33,34,47,48] However, the application of single-column separation of Li can be largely limited by high cumulative procedural blanks, the tailing of Li peaks, and incomplete Li recovery and subsequent column-induced isotopic fractionation.[42] To achieve satisfactory separation of Li/matrix elements, large resin loads, high aspect ratios, and large eluent volumes are required.[3] In addition, significant Li peak

Table 2 Instrumental operating conditions and data acquisition parameters

Equipment model	Agilent Technologies™ 7900 (this study)	Agilent Technologies™ 7900cs (Misra and Froelich, 2009)[42]
Instrumental operating conditions		
RF power (W)	1550 (hot plasma)	600 (cool plasma)
RF maching (V)	1.58	—
Nebulizer	Concentric (PFA) self aspirating	Concentric (PFA) self aspirating
Sample uptake rate (μL min^{-1})	~200 μL min^{-1}	~100 μL min^{-1}
Guard electrode	On	—
Sampling depth (mm)	6.8	6.5 to 7.5
Spray chamber	Quartz	Quartz
Spray chamber temperature (°C)	2	2
Cool Ar gas flow rate (L min^{-1})	15	—
Carrier Ar gas flow rate (L min^{-1})	0.95	0.60 to 0.65
Make-up Ar gas flow rate (L min^{-1})	0.35	0.30 to 0.40
Sampler cone	Nickel	Platinum
Skimmer cone	Nickel	Platinum
1st extraction lens (V)	−110	−120 to −130
2nd extraction lens (V)	−116.5	−10 to −5
Omega lens (V)	7.8	—
Omega bias (V)	−19	—
Integration time (s)	13 s (^{6}Li) and 1 s (^{7}Li)	13 s (^{6}Li) and 1 s (^{7}Li)
Nebulizer pump (rps)	0.1	—
Sample uptake time (s)	45	60
Stabilization time (s)	30	—
Measurement time (s)	50	—
Pulse detection limit (cps)	1.0×10^6	3.0×10^6
Wash-out time (s)	180 (rinse 1: 75; rinse 2: 45; rinse 3: 60)	240

migrations generally occur due to changes in matrix load and elution matrix strength. Here we used a modified dual-column procedure to achieve fixed Li elution peaks with complete separation from matrix Na. Using 0.7 mol L^{-1} HNO_3 as the elution acid in the first step columns, high ionic potential cations such as Fe^{3+} and Al^{3+} were retained by the resin, but low ionic potential cations (*i.e.*, Li^+, Na^+ and K^+) with low partition coefficients went directly through. Li is the first element to elute off from the columns with 30 to 80 mL elution acid within 50 mL of the total elution volume (Fig. 1). Both pre-cuts and post-cuts have negligible amounts of Li. Sodium, the next element to elute after Li, emerges after 52 mL of elution. Not surprisingly, a complete separation between lithium and sodium cannot be achieved with the first column, requiring the second column for further purification of Li from Na. Using 0.2 mol L^{-1} HCl in the second chromatographic step, Li fractions are in the 32 to 60 mL elution fraction within 28 mL of the total elution volume, completely separated from Na. Low blanks of both pre-Li and post-Li fractions demonstrate the absence of Li breakthrough or tailing of elution peaks.

The compositionally diverse geological samples yield analogous elution curves (Fig. 1), proving that this method is widely suitable for samples with various matrix compositions. In comparison with single-column systems, the most significant advantage of this dual-column system is the high loading capacity for low-Li samples and consistent elution range of the Li cuts for geomaterials with various matrix compositions, eliminating the need for repeated chromatography, material-specific column systems[33] and elution curve recalibration.[3] The low cumulative Li blank, high loading capacity and fixed Li elution range are key features of our method, particularly suitable for low-Li sized and high-matrix geological samples. The Li yields of samples after column chemistry can be determined by collecting pre- and post-cuts in addition to Li cuts. We have checked our Li column yields by comparing Li cuts with the sum of Li cuts, and pre- and post-cuts to ensure ~100% Li recovery (Table 3).

Precision and accuracy

Short-term and long-term stability. The precision and accuracy of our analytical procedure were evaluated by repeated analyses of pure Li reference solutions (IRMM-016), as well as two USGS rock standards (BCR-2 and JG-2). To account for the instrumental drift and mass bias, short-term examination bracketed by the IRMM-016 Li standard was performed. As discussed above, we measured each sample 5–8 times and reported the averages of repeat measurements. The short-term stability (2SD) of the Q-ICP-MS method is 1.6‰ for the IRMM-016 solution, 1.1‰ for the BCR-2 basalt standard and 1.7‰ for the JG-2 granite standard, respectively. To evaluate the long-term reproducibility, two geostandards BCR-2 and JG-2 in addition to the IRMM-016 standard were routinely measured over a period of 10 months (Fig. 2). During the 10 month period from April 2018 to January 2019, the averaged δ^7Li was 3.1‰ for BCR-2 and 0.2‰ for JG-2, with the long-term external two standard deviations (2SD) of 1.1‰ and 1.0‰, respectively. We

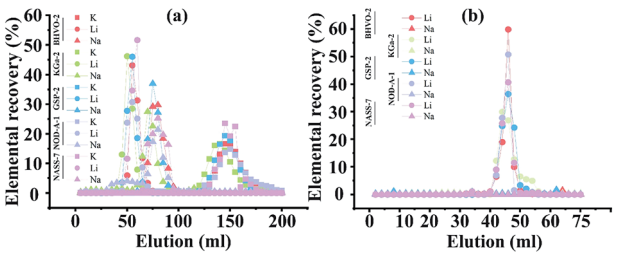

Fig. 1 Column elution curves for multiple geostandards. (a) Fat column 1 in 0.7 mol L^{-1} HNO_3; (b) thin column 2 in 0.2 mol L^{-1} HCl. See the text for details.

Table 3 Lithium recovery and Na/Li ratios before and after isolation of the thirteen geostandards

Separation method	Sample	Type	Li mass added (ng)	Li mass collected (ng)	Li recovery (%)	Final Na/Li mass ratio
Dual-column chromatography	NIST-SRM-Id	Limestone	84.4	83.2	98.6	0.4
	JCP-1	Coral	40.6	40.8	100.5	0.3
	GSP-2	Granodiorite	649.2	651.0	100.3	0.1
	BHVO-2	Basalt	70.0	69.8	99.7	0.9
	BCR-2	Basalt	81.0	82.0	101.2	0.5
	JB-2	Basalt	488.6	487.8	99.8	0.4
	JG-2	Granite	423.2	423.0	100.0	0.5
	KGa-2	Clay (kaolinite)	351.2	347.6	99.0	0.1
	Swy-3	Clay (smectite)	371.8	367.0	98.7	0.0
	IMt-2	Clay (illite)	307.2	308.2	100.4	0.5
	SBC-1	Shale	1084.6	1078.6	99.5	1.0
	NASS-7	Seawater	919.0	913.6	99.4	1.0
	NOD-A-1	Marine Mn nodules	713.4	720.4	101.0	0.3

take the 2SD range from these long-term standard analyses as a representative value for the bracketing standards during one analytical session. Based on these results, the long-term external reproducibility of our analytical routine is conservatively estimated to be better than 1.1‰, comparable to that (1.1‰) reported in a recent MC-ICP-MS study.[49]

Application to the reference materials. The whole-procedure accuracy of our analytical routine can be validated by the comparable results obtained between our and other laboratories for 13 chemically diverse natural geological standards with different matrix compositions (Table 4). In addition, we also report the Li isotope data of IRMM-016 after column chemistry to validate our chromatography method. The results from three basaltic references, BHVO-2 (4.7 ± 0.57‰, n = 10), BCR-2 (3.16 ± 1.10‰, n = 10), and JB-2 (4.56 ± 0.56‰, n = 10), are consistent with published data, within analytical error. The average δ^7Li values measured for two granitic standards, JG-2 (0.25 ± 1.02‰, n = 54) and GSP-2 (−0.56 ± 0.72‰, n = 54), are in agreement with published data.[6,27,34,35,50,51] The carbonate standard JCP-1 yields δ^7Li values of 19.83 ± 1.07‰ (n = 10), which are slightly lower than the reported data (20.16–20.27‰),[29,31] but within uncertainty. Clay Swy-3 (smectite), KGa-2 (kaolinite) and IMt-2 (illite) present δ^7Li values of −0.58 ± 0.36‰ (n = 10), 0.16 ± 0.69‰ (n = 10) and 5.95 ± 0.68‰ (n = 10). These results are consistent with the reported data.[18] The Li isotope compositions in three sedimentary geostandards, carbonate NIST-SRM-1d, manganese nodule NOD-A-1 and shale SBC-1, are 6.07 ± 1.20‰ (n = 10), 26.85 ± 1.30‰ (n = 10) and 0.23 ± 0.90‰ (n = 10) respectively, agreeing well with our previous study (*i.e.*, SBC-1, 5.63 ± 0.48‰, n = 4; NOD-A-1, 0.29 ± 0.23‰, n = 3).[35]

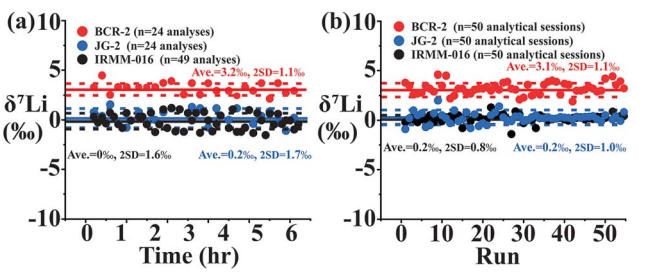

Fig. 2 Short-term (a) and long-term (b) instrumental stability and precision of Li isotope analysis (δ^7Li) with respect to the IRMM-016 Li carbonate standard and igneous geostandards (BCR-2 and JG-2) purified through column chemistry. The instrumental stability was determined by back-to-back runs of 0.5 ppb IRMM-016 in 2% HNO_3 (v/v). The dashed lines represent the 2SD uncertainty of multiple sample measurements in the short term (~6 h) and long term (10 months) as the expected external precision. The solid lines represent the average value of multiple sample measurements. The long-term external precision (2SD) of the instrument is 0.8‰ for the IRMM-016 Li reference, and 1.0‰ and 1.1‰ for the BCR-2 basalt standard and JG-2 granite standard, respectively.

Because of the long residence time in the open ocean (~1.5 Ma)[50] compared to the ocean mixing time (~1 kyr), Li is a conservative element with homogeneous elemental and isotopic compositions.[23,52–54] Using a Q-ICP-MS instrument, Misra and Froelich (2009)[42] reported an overall seawater δ^7Li ratio of 30.75 ± 0.41‰ (n = 10), identical to the average published value of 31.0 ± 0.5‰.[2] In this study, the seawater standard NASS-7 yields an average δ^7Li of 30.42 ± 0.97‰ (n = 3), consistent with the results of our recent work using a MC-ICP-MS[35] and the published values for seawater standards NASS-5 and NASS-6 (29.6–30.87‰).[28–30,34,55,56] In addition, an aliquot of the Li standard solution (IRMM-016) was processed through column chemistry, whose δ^7Li values (0.16 ± 0.83‰) agreed with our long-term average value of 0.15‰ (Fig. 2) without column chemistry within our precision. To establish the validity of this method, the values obtained from separately digested materials in different measurement sessions over a period of ten months by our Q-ICP-MS method also confirm a long-term consistency and external reproducibility. In summary, there is no systematic shift found between data from Q-ICP-MS (this study), TIMS and MC-ICP-MS from different laboratories (Table 4). Therefore, we listed the measured data in this study as acceptable reference values, and recommend them for future inter-laboratory comparison.

Optimization of Li isotope analysis

This section provides detailed information on how to achieve routine high precision and accuracy Li isotope analysis using a Q-ICP-MS through optimization of various parameters.

Table 4 Measured Li isotope ratios and reported data in reference materials

Reference material	Type	Source	Reference	δ^7Li (‰)	2SD	Instrument	Reference material		Source	Reference	δ^7Li (‰)	2SD	Instrument
BHVO-1	Basalt	USGS	50	5.8	—	TIMS	JG-2	Granite	GSJ	34	0.15	0.15	MC-ICP-MS
BHVO-1			59	4.61	—	MC-ICP-MS	JG-2			51	0	0.2	MC-ICP-MS
BHVO-1			60	5.2	—	TIMS	JG-2			27	0.24	0.2	MC-ICP-MS
BHVO-1			6	5.5	0.6	MC-ICP-MS	JG-2			6	−0.7	0.4	MC-ICP-MS
BHVO-1			6	4.7	0.4	MC-ICP-MS	JG-2			50	0.4	0.1	TIMS
BHVO-1			10	5	1.5	MC-ICP-MS	JG-2			35	0.32	0.31	MC-ICP-MS
BHVO-1			7	4.3	—	MC-ICP-MS	JG-2			This study	0.25	1.02	Q-ICP-MS
BHVO-2			28	4.38	0.16	MC-ICP-MS	GSP-2	Granite	USGS	34	−0.78	0.25	MC-ICP-MS
BHVO-2			34	4.5	0.24	MC-ICP-MS	GSP-2			65	−0.8	0.3	MC-ICP-MS
BHVO-2			30	4.46	0.37	MC-ICP-MS	GSP-2			35	−0.56	0.55	MC-ICP-MS
BHVO-2			27	4.66	0.22	MC-ICP-MS	GSP-2			This study	−0.56	0.72	Q-ICP-MS
BHVO-2			48	4.29	0.23	MC-ICP-MS	IRMM-016	Lithium carbonate	IRMM	34	0	0.16	MC-ICP-MS
BHVO-2			29	4.63	0.16	MC-ICP-MS	IRMM-016			56	0.2	0.3	MC-ICP-MS
BHVO-2			61	4.8	0.3	MC-ICP-MS	IRMM-016			66	0.1	0.4	MC-ICP-MS
BHVO-2			62	4.9	0.8	MC-ICP-MS	IRMM-016			51	0.2	0.2	MC-ICP-MS
BHVO-2			35	4.63	0.29	MC-ICP-MS	IRMM-016			54	0.2	0.24	MC-ICP-MS
BHVO-2			This study	4.7	0.57	Q-ICP-MS	IRMM-016			27	0.14	0.04	Q-ICP-MS
BCR-1	Basalt	USGS	51	2.5	0.5	MC-ICP-MS	IRMM-016			This study	0.16	0.83	Q-ICP-MS
BCR-1			44	2.38	0.52	MC-ICP-MS	NASS-5	Seawater	NRCC	30	30.55	0.45	MC-ICP-MS
BCR-1			17	2	0.7	MC-ICP-MS	NASS-5			55	30.29	0.65	MC-ICP-MS
BCR-2			30	2.84	0.45	MC-ICP-MS	NASS-5			28	30.64	0.44	MC-ICP-MS
BCR-2			28	2.87	0.39	MC-ICP-MS	NASS-5			29	30.72	0.17	MC-ICP-MS
BCR-2			29	2.6	0.3	MC-ICP-MS	NASS-6			34	30.87	0.15	MC-ICP-MS
BCR-2			31	2.82	0.13	MC-ICP-MS	NASS-6			56	29.6	2.2	MC-ICP-MS
BCR-2			35	3.02	0.51	MC-ICP-MS	NASS-6			62	31.3	0.9	MC-ICP-MS
BCR-2			This study	3.16	1.1	Q-ICP-MS	NASS-7			35	30.42	0.97	Q-ICP-MS
JB-2	Basalt	GSJ	24	4.9	0.7	TIMS	NASS-7			This study	30.63	1.31	Q-ICP-MS
JB-2			25	5.1	1.2	MC-ICP-MS	NIST-SRM-1d	Carbonate	NIST	35	5.63	0.48	MC-ICP-MS
JB-2			50	6.8	—	TIMS	NIST-SRM-1d			This study	6.07	1.2	Q-ICP-MS
JB-2			47	4.3	0.3	MC-ICP-MS	JCP-1	Carbonate (coral)	GSJ	29	20.16	0.2	MC-ICP-MS
JB-2			6	3.9	0.4	MC-ICP-MS	JCP-1			31	20.27	0.41	MC-ICP-MS
JB-2			14	4.7	—	MC-ICP-MS	JCP-1			35	19.56	0.53	MC-ICP-MS
JB-2			27	4.3	0.26	MC-ICP-MS	JCP-1			This study	19.83	1.07	Q-ICP-MS
JB-2			44	4.7	0.29	MC-ICP-MS	NOD-A-1	Manganese nodule	USGS	35	26.31	0.97	MC-ICP-MS
JB-2			7	4	—	MC-ICP-MS	NOD-A-1			This study	26.85	1.3	Q-ICP-MS
JB-2			63	5.2	—	MC-ICP-MS	Swy-1	Smectite	CMS	18	5.9	—	MC-ICP-MS
JB-2			29	4.31	0.69	MC-ICP-MS	Swy-3			This study	−0.58	0.36	Q-ICP-MS
JB-2			64	5.1	0.4	TIMS	KGa-2	Kaolinite	CMS	18	0.1	—	MC-ICP-MS
JB-2			35	4.71	0.23	MC-ICP-MS	KGa-2			35	0.15	0.04	MC-ICP-MS
JB-2			This study	4.56	0.56	Q-ICP-MS	KGa-2			This study	0.16	0.69	Q-ICP-MS
SBC-1	Shale	USGS	35	0.29	0.03	MC-ICP-MS	IMt-1	Illite	CMS	18	2.5	—	MC-ICP-MS
SBC-1			This study	0.23	0.9	Q-ICP-MS	IMt-2			This study	5.95	0.68	Q-ICP-MS

RF power: hot plasma *vs.* cool plasma. The choice of RF power reflects a balance between the ionization efficiency and amount of interference. Previous studies have adopted two plasma powers to achieve high precision Li isotope analysis: cool plasma[42] and hot plasma conditions.[40] The major advantage of cool plasma conditions is that lithium with low first ionization potential is almost completely ionized while formation of oxides and doubly charged ions is minimized. Moreover, under cool plasma conditions, ionization of other matrix-based high first ionization potential interference is significantly reduced. The hot plasma conditions have the advantage of higher plasma stability and sensitivity. Therefore, we tested cool plasma (600 W) and hot plasma (1550 W) conditions to optimize RF power for Li isotope analysis. We tuned the ICP-MS to maximize lithium sensitivity and signal stability in both cool and hot plasma settings, respectively.

Compared with the cool plasma conditions, the hot plasma settings demonstrate better external precision of ±1.1‰ (2SD) (Fig. 3). A possible reason may be that accurate Li isotope ratio determination by ICP-MS is sensitive to the presence of matrix elements, especially in the cold plasma.[26] To minimize the plasma-based argon ionization in the central channel and doubly charged $^{12}C^{2+}$ and $^{14}N^{2+}$ interference on $^{6}Li^{+}$ and $^{7}Li^{+}$, Misra and Froelich (2009)[42] used cool plasma conditions (600 W) with an Agilent™ 7500 Q-ICP-MS. Cool plasma has its advantages because of its lower background for Li. However, the content of oxides is usually high under cool plasma conditions, creating possible matrix effects.

Acid molarity matching. The uncertainty associated with differences in the molarity of concentrated acids, and volume and weight measurements, as well as occasional artifacts (*e.g.*, operation miss and evaporation) may change the final acid molarity. The mismatch in acid molarity between samples and bracketing standards could introduce significant shifts in space charge effects. Such influence could cause differential instrumental mass bias between samples and their bracketing standards, resulting in measurable differences in isotopic ratios. These offsets have been observed for K, Mg and Fe isotope systems.[56–58] The effect of such a mismatch on Li isotope analysis by Q-ICP-MS has not, to our knowledge, been reported. To investigate possible impacts of acid mismatch on Li isotope analysis, pure IRMM-016 solutions of 0.5 ppb Li in 1–5% HNO_3 (v/v) were tested against the same solutions in 2% HNO_3 (v/v). Interestingly, the results demonstrated a positive correlation between the δ^7Li values of the sample and how well its concentration matches the bracketing standard (Fig. 4). The 0.5 ppb IRMM-016 in 2% HNO_3 (v/v) solutions bracketed by themselves yielded δ^7Li values between −0.01‰ and 0.01‰, consistent with the expected value of 0‰. However, both low and high acid molarity with respect to the bracketing solutions produced large drifts, up to ~8‰ in Li isotope analysis. Our tests on the Q-ICP-MS showed that acid mismatches can significantly affect the accuracy of Li isotope analysis. As such, one needs to match the acid molarity of samples and standards.

Concentration matching. Instrumental mass bias could be significant and fluctuate with time, thus reducing the accuracy and precision of isotopic measurement. Here a standard–sample bracketing method was used by assuming that the instrumental mass bias for the sample and standard is the same. This requires that the sample and standard have identical Li concentrations. First, we tested the lower Li threshold of isotopic measurement for the optimization of low-size samples. Apparently, Li concentration selection in the range of 0.1–5 ppb can introduce small, but measurable errors in Li isotope data acquisition by Q-ICP-MS (Fig. 5). The isotopic response to increasing Li concentration is invariant in the 0.5 ppb to 5 ppb range, within the external precision (2SD = ±1.1‰). This amount of Li required for a single Q-ICP-MS analysis (0.5 ng) is almost an order of magnitude smaller than the amounts required by previous MC-ICP-MS methods.[25–28,54] There is a decreasing stability of Li isotope analysis with Li concentration down to 0.1–0.25 ppb, probably due to the insufficient detection sensitivity.

The Li concentration mismatch between the sample and its bracketing standards may influence the accuracy of Li isotope analysis. Such effects on Li isotope measurement were evaluated by testing Li concentration mismatched (between 80 and 150%) IRMM-016 standards bracketed with the same 0.5 ppb Li standard. The results depicted in Fig. 5 demonstrate systematic δ^7Li offsets for mismatches in Li concentration between

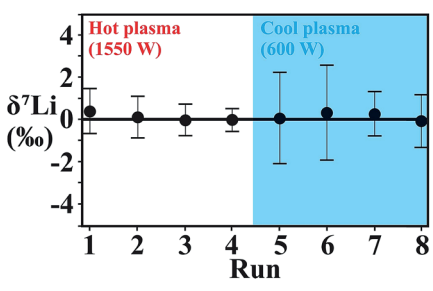

Fig. 3 Multiple analyses of pure Li solutions (IRMM-016, 0.5 ppb Li) under hot (1550 W) and cool (600 W) plasma conditions. The solid line stands for the expected IRMM-016 δ^7Li = 0‰. Error bars represent the analytical uncertainty (2SD) of more than five repeated sample analyses.

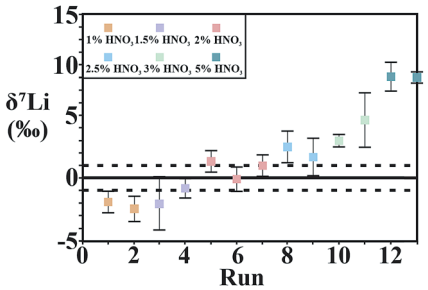

Fig. 4 Effects of acid molarity mismatches on Li isotope measurement by Q-ICP-MS. All measurements were bracketed by 0.5 ppb Li standard IRMM-016 in 2% HNO_3 (v/v). The solid line stands for the expected IRMM-016 δ^7Li = 0‰. The dashed lines represent the long-term 2SD of multiple sample measurements as external precision. Error bars represent the analytical uncertainty (2SD) of more than fiver repeated sample analyses.

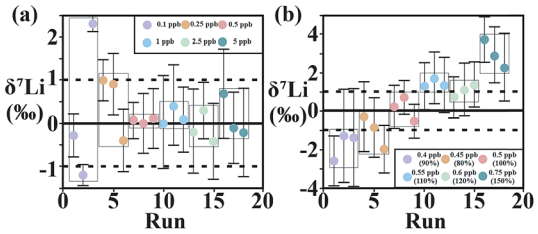

Fig. 5 Effects of (a) Li concentrations and (b) concentration mismatch between aliquots and bracketing standards on Li isotope measurement by Q-ICP-MS. The Li concentrations of samples and standards are controlled at 0.5 ppb and within 5% for all measurements conducted to ensure precision and accuracy. The solid line stands for the expected IRMM-016 δ^7Li = 0‰. The dashed lines represent the long-term 2SD of multiple sample measurements as external precision. Error bars show the analytical uncertainty (2SD) of over five repeated sample analyses.

samples and standards. According to our results, a Li concentration mismatch would result in an observable deviation when the sample and standard concentration mismatch is more than 10%. Therefore, we recommend that Li concentrations in samples and standards be matched within 5% to guarantee precision and accuracy.

Evaluation of matrix effects. The matrix effect of Na (the most common matrix element) on Li isotope analysis is evaluated, and it could change the instrumental mass bias, violating the prerequisite for applying the standard–sample–standard bracketing method.[25] Due to the small differences in the partition coefficients between Li and Na, the tailing of Na peaks in Li fractions is common during column purification, especially for Na-enriched geological samples like seawater and brines. Therefore, a two-step chromatographic separation is commonly adopted for Li purification from matrix elements, especially for Na.[35] Nonetheless, we investigated the influence of the presence of Na on Li isotope measurements. Systematic investigations on Li isotope measurement techniques revealed that significant interference of Na in sample solutions degrades the accuracy of Li isotope composition determinations, and the results are shown in Fig. 6. Generally, matrix-induced mass bias (Na/Li = 20) can cause a decrease in δ^7Li values by up to 3‰,[27,47] potentially related to peak ionization delay.[26] In contrast, both Bryant *et al.* (2003)[26] and our recent work[35] demonstrated that high Na/Li ratios could induce a δ^7Li increase by ~1‰. The increase in δ^7Li due to a high Na/Li ratio in the test solution is consistent with our current understanding of the space charge effects. In the presence of Na^+, the light Li isotope ($^6Li^+$) should be preferentially expelled, thus increasing the detected ^{7}Li/^{6}Li ratios. It seems that spectral matrix effects could cause signal enhancement or suppression in different instrument settings, and are not a linear function of Na/Li (Fig. 6). Therefore, we speculate that this deviation in δ^7Li is complex, and may be linked to differences in various instrumental conditions.

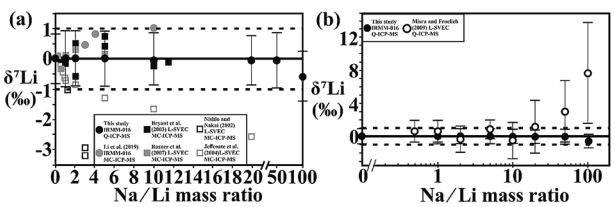

Fig. 6 Assessment of the influence of Na on Li isotope measurements with Na : Li molar ratios varying from 0 to 100. (a) Comparison between Q-ICP-MS and MC-ICP-MS data. (b) Comparison of Q-ICP-MS data reported in Misra and Froelich (2009) and this study. The δ^7Li data was the average value of over five replicate analyses. The solid line stands for IRMM-016 δ^7Li = 0‰. The dashed lines represent the long-term 2SD of sample analysis by Q-ICP-MS. Error bars represent the analytical uncertainty (2SD) of over five repeated sample analyses. Some uncertainties of reference data of MC-ICP-MS methods are not shown.

Complete removal of Na must be guaranteed for TIMS and MC-ICP-MS analyses. To examine the effect of Na on Li isotope measurement, we used a series of mixed solutions (0.5 ppb Li, IRMM-016) doped with various amounts of Na (Na/Li mass ratios from 0.5 to 100). In contrast to results from MC-ICP-MS analysis, our results show that the presence of Na standards with Na/Li mass ratios up to 50 does not affect the accuracy of the measured δ^7Li values. A decrease of 0.6‰ in the measured δ^7Li occurs when the Na/Li ratio reaches 100, although it is still within our reported analytical uncertainty of 2SD = ±1.1‰. High-resolution TIMS and MC-ICP-MS techniques require ultra-clean Li solutions to eliminate matrix-induced mass bias.[3] However, our results show large matrix tolerance of the Q-ICP-MS method. Thus, our Q-ICP-MS method with hot plasma is more resistant to matrix interference. The Q-ICP-MS technique is more robust in terms of matrix tolerance compared to TIMS and MC-ICP-MS methods, especially for samples with high Na/Li ratios.[28,41] Therefore, if the Na/Li ratios in samples are less than 100, column chemistry is unnecessary for the designed Q-ICP-MS approach.

Conclusions

We have developed an efficient mass spectrometric protocol for routine and accurate determination of Li isotope ratios using an Agilent™ 7900 single collector Q-ICP-MS. The method shows comparable long-term precision (2SD = ±1.1‰) and accuracy to TIMS and MC-ICP-MS techniques. Our analytical approach allows for low mass consumption (2.5 ng/quintuplicate analyses), a low whole-procedure blank and high matrix tolerance (Na/Li ~ 100), pushing the boundary for Li isotope investigation of geological materials. We also presented a detailed dual-column Li purification protocol. This dual-column system has two advantages: (1) it enables high loading capacity (29.6 meq), complete recovery (~100%) and satisfactory purification (Na/Li < 1) of Li. (2) The dual-column isolation routinely achieved a fixed elution range of Li cuts (32–60 mL 0.2 mol L^{-1} HCl), preventing re-calibration of columns for geologically diverse matrix variations. Furthermore, washing with 1% HF + 2% HNO_3 (v/v), and then 1% HNO_3 + 5% HCl (v/v), and 2% HNO_3 (v/v) in between analyses can significantly minimize the memory effect of Li. The newly developed chromatography and Q-ICP-MS techniques can be applied to chemically diverse materials, and is particularly optimized for ng-sized and high-matrix level

geological samples such as seawater and brines. We reported accurate and reproducible Li isotope measurements in various geostandards, including seawater (NASS-7), igneous rocks (BHVO-2, BCR-2, JG-2, JB-2 and GSP-2), biogenetic/abiogenic carbonates (IRMM-016, JCP-1 and NIST-SRM-1d), a marine manganese nodule (NOD-A-1), shale (SBC-1) and clay minerals (KGa-2, IMt-2 and SWy-3). Our δ^7Li results agree with published data, and therefore our findings serve as reference values for quality control and inter-laboratory calibration.

Author contributions

X.-M. L. and W. L. contributed equally to this work.

Conflicts of interest

There are no conflicts to declare.

Acknowledgements

We would like to thank Bert Woods and Mark Kelinske for their help with the optimization of Q-ICP-MS for isotope analysis. Cheng Cao, Ryan Mills and Drew Coleman are thanked for their help at the Isotope Geochemistry Lab at UNC. The manuscript benefited from the comments of two anonymous reviewers and the efficient handling of the editor. We acknowledge funding support from an NSF Career Award (EAR-1848153) and the University of North Carolina. This research is supported by the US Army Research Office under grant W911NF-17-2-0028. The views and conclusions contained in this document are those of the authors, and should not be interpreted as representing the official policies, either expressed or implied, of the sponsors, including the Army Research Laboratory or the U.S. Government. The U.S. Government is authorized to reproduce and distribute reprints for Government purposes notwithstanding any copyright notation herein.

References

1 L. H. Chan, in *Handbook of Stable Isotope Analytical Techniques*, 2004, pp. 122–141.
2 P. B. Tomascak, in *Reviews in Mineralogy and Geochemistry*, 2004, pp. 153–195.
3 P. B. Tomascak, T. Magna, and R. Dohmen, in *Advances in Lithium Isotope Geochemistry*, 2016.
4 S. Penniston-Dorland, X. M. Liu and R. L. Rudnick, in *Reviews in Mineralogy and Geochemistry*, 2017, pp. 165–217.
5 Y. Huh, C. H. Chan and O. A. Chadwick, *Geochem., Geophys., Geosyst.*, 2004, **5**, Q09002.
6 J. S. Pistiner and G. M. Henderson, *Earth Planet. Sci. Lett.*, 2003, **214**, 327–339.
7 R. L. Rudnick, P. B. Tomascak, H. B. Njo and L. R. Gardner, *Chem. Geol.*, 2004, **212**, 45–57.
8 L. H. Chan and M. Kastner, *Earth Planet. Sci. Lett.*, 2000, **183**, 275–290.
9 R. H. James, D. E. Allen and W. E. Seyfried Jr, *Geochim. Cosmochim. Acta*, 2003, **67**, 681–691.
10 C. Bouman, T. Elliott and P. Z. Vroon, *Chem. Geol.*, 2004, **212**, 59–79.
11 L. B. Williams and R. L. Hervig, *Geochim. Cosmochim. Acta*, 2005, **69**, 5705–5716.
12 L. D. Benton, J. G. Ryan and I. P. Savov, *Geochem., Geophys., Geosyst.*, 2004, **5**, Q08J12.
13 F. Z. Teng, W. F. McDonough, R. L. Rudnick and B. A. Wing, *Chem. Geol.*, 2007, **239**, 1–12.
14 T. Zack, P. B. Tomascak, R. L. Rudnick, C. Dalpé and W. F. McDonough, *Earth Planet. Sci. Lett.*, 2003, **208**, 279–290.
15 C. C. Lundstrom, M. Chaussidon, A. T. Hsui, P. Kelemen and M. Zimmerman, *Geochim. Cosmochim. Acta*, 2005, **69**, 735–751.
16 F. M. Richter, A. M. Davis, D. J. vDePaolo and E. B. Watson, *Geochim. Cosmochim. Acta*, 2003, **67**, 3905–3923.
17 F. Z. Teng, W. F. McDonough, R. L. Rudnick and R. J. Walker, *Earth Planet. Sci. Lett.*, 2006, **243**, 701–710.
18 P. H. Tsai, C. F. You, K. F. Huang, C. H. Chung and T. B. Sun, *Asian J. Earth Sci.*, 2014, **87**, 1–10.
19 L. Sauzéat, R. L. Rudnick, C. Chauvel, M. Garçon and M. Tang, *Earth Planet. Sci. Lett.*, 2015, **428**, 181–192.
20 J. S. Harkness, N. R. Warner, A. Ulrich, R. Millot, W. Kloppmann, J. M. Ahad, M. M. Savard, P. Gammon and A. Vengosh, *Appl. Geochem.*, 2018, **90**, 50–62.
21 L. H. Chan, *Anal. Chem.*, 1987, **59**, 2662–2665.
22 T. Moriguti and E. Nakamura, *Proc. Jpn. Acad., Ser. B*, 1993, **69**, 123–128.
23 C. F. You and L. H. Chan, *Geochim. Cosmochim. Acta*, 1996, **60**, 909–915.
24 T. Moriguti and E. Nakamura, *Chem. Geol.*, 1998, **145**, 91–104.
25 P. B. Tomascak, R. W. Carlson and S. B. Shirey, *Chem. Geol.*, 1999, **158**, 145–154.
26 C. J. Bryant, M. T. McCulloch and V. C. Bennett, *J. Anal. At. Spectrom.*, 2003, **18**, 734–737.
27 A. B. Jeffcoate, T. Elliott, A. Thomas and C. Bouman, *Geostand. Geoanal. Res.*, 2004, **28**, 161–172.
28 M. Rosner, L. Ball, B. Peucker-Ehrenbrink, J. Blusztajn, W. Bach and J. Erzinger, *Geostand. Geoanal. Res.*, 2007, **31**, 77–88.
29 K. F. Huang, C. F. You, Y. H. Liu, R. M. Wang, P. Y. Lin and C. H. Chung, *J. Anal. At. Spectrom.*, 2010, **25**, 1019–1024.
30 M. S. Choi, J. S. Ryu, H. Y. Park, K. S. Lee, Y. Kil and H. S. Shin, *J. Anal. At. Spectrom.*, 2013, **28**, 505–509.
31 M. S. Bohlin, S. Misra, N. Lloyd, H. Elderfield and M. J. Bickle, *Rapid Commun. Mass Spectrom.*, 2018, **32**, 93–104.
32 D. Kutscher, J. D. Wills and S. M. Ducos, *Technical Note TN43202*, Bremen, Germany, 2014.
33 K. Van Hoecke, J. Belza, T. Croymans, S. Misra, P. Claeys and F. Vanhaecke, *J. Anal. At. Spectrom.*, 2015, **30**, 2533–2540.
34 J. Lin, Y. Liu, Z. Hu, L. Yang, K. Chen, H. Chen, K. Zong and S. Gao, *J. Anal. At. Spectrom.*, 2016, **31**, 390–397.
35 W. Li, X. Liu and L. V. Godfrey, *Geostand. Geoanal. Res.*, 2019, **43**, 261–276.
36 J. Vogl, *Inductively Coupled Plasma Mass Spectrometry Handbook*, Blackwell Publishing Ltd., Oxford, 2005, pp. 147–181.

37 J. Meija, L. Yang, Z. Mester and B. E. Sturgeon, *Isotopic Analysis*, Wiley-VCH Verlag GmbH & Co, KGaA, 2012, pp. 113–137.
38 X. F. Sun, B. T. G. Ting, S. H. Zeisel and M. Janghorbani, *Analyst*, 1987, **112**, 1223–1228.
39 H. Vanhoe, C. Vandecasteele, J. Versieck and R. Dams, *Anal. Chim. Acta*, 1991, **244**, 259–267.
40 D. C. Grégoire, B. M. Acheson and R. P. Taylor, *J. Anal. At. Spectrom.*, 1996, **11**, 765–772.
41 M. K. Košler and P. Sylvester, *Chem. Geol.*, 2001, **181**, 169–179.
42 S. Misra and P. N. Froelich, *J. Anal. At. Spectrom.*, 2009, **24**, 1524–1533.
43 G. D. Flesh, A. R. Anderson and H. J. Svec, *Int. J. Mass Spectrom.*, 1973, **12**, 265–272.
44 T. Magna, U. H. Wiechert and A. N. Halliday, *Int. J. Mass Spectrom.*, 2004, **239**, 67–76.
45 Y. Hu, X. Y. Chen, Y. K. Xu and F. Z. Teng, *Chem. Geol.*, 2018, **493**, 100–108.
46 H. Chen, Z. Tian, B. Tuller-Ross, R. L. Korotev and K. Wang, *J. Anal. At. Spectrom.*, 2019, **34**, 160–171.
47 Y. Nishio and S. I. Nakai, *Anal. Chim. Acta*, 2002, **456**, 271–281.
48 Y. Gao and J. F. Casey, *Geostand. Geoanal. Res.*, 2012, **36**, 75–81.
49 R. S. Hindshaw, R. Tosca, T. L. Goût, I. Farnan, N. J. Tosca and E. T. Tipper, *Geochim. Cosmochim. Acta*, 2019, **250**, 219–237.
50 R. H. James and M. R. Palmer, *Chem. Geol.*, 2000, **166**, 319–326.
51 T. T. Phan, R. C. Capo, B. W. Stewart, G. L. Macpherson, E. L. Rowan and R. W. Hammack, *Chem. Geol.*, 2016, **420**, 162–179.
52 Y. Huh, L. H. Chan, L. Zhang and J. M. Edmond, *Geochim. Cosmochim. Acta*, 1998, **62**, 2039–2051.
53 L. H. Chan and J. M. Edmond, *Geochim. Cosmochim. Acta*, 1988, **52**, 1711–1717.
54 R. Millot, C. Guerrot and N. Vigier, *Geostand. Geoanal. Res.*, 2004, **28**, 153–159.
55 M. S. Choi, H. S. Shin and Y. W. Kil, *Microchem. J.*, 2010, **95**, 274–278.
56 S. Pfister, R. C. Capo, B. W. Stewart, G. L. Macpherson, T. T. Phan, J. B. Gardiner, J. R. Diehl, C. L. Lopano and J. A. Hakala, *Appl. Geochem.*, 2017, **87**, 122–135.
57 N. Dauphas, A. Pourmand and F. Z. Teng, *Chem. Geol.*, 2009, **267**, 175–184.
58 F. Z. Teng and W. Yang, *Rapid Commun. Mass Spectrom.*, 2014, **28**, 19–24.
59 *Thermo Finnigan Report NEPTUNE Thermo Finnigan Application Flash Report*, No. N2, 2001, p. 2.
60 L. H. Chan and F. A. Frey, *Geochem., Geophys., Geosyst.*, 2003, **4**, 8707.
61 T. Elliott, A. Thomas, A. Jeffcoate and Y. Niu, *Nature*, 2006, **443**, 565.
62 P. A. P. Pogge von Strandmann, K. W. Burton, R. H. James, P. van Calsteren and S. R. Gislason, *Chem. Geol.*, 2010, **270**, 227–239.
63 H. M. Seitz, G. P. Brey, Y. Lahaye, S. Durali and S. Weyer, *Chem. Geol.*, 2004, **212**, 163–177.
64 L. H. Chan, W. P. Leeman and C. F. You, *Chem. Geol.*, 2002, **182**, 293–300.
65 H. Sun, Y. Gao, Y. Xiao, H. O. Gu and J. F. Casey, *Chem. Geol.*, 2016, **439**, 71–82.
66 G. L. Macpherson, R. C. Capo, B. W. Stewart, T. T. Phan, K. Schroeder and R. W. Hammack, *Geofluids*, 2014, **14**, 419–429.